Structure and Infrared Spectroscopy of Group 6 Transition-Metal Carbonyls in the Gas Phase: DFT Studies on M(CO)$_n$ (M = Cr, Mo, and W; n = 6, 5, 4, and 3)

Yo-ichi Ishikawa* and Kenta Kawakami

Department of Chemistry and Materials Technology, Kyoto Institute of Technology, Matsugasaki, Sakyo-ku, Kyoto 606-8585, Japan

Received: February 22, 2007

B3LYP-based density functional theory (DFT) calculations with effective core potentials (ECPs) (LANL2DZ) on M and 6-311+G(2d) all-electron basis function sets on C and O are used to interpret the symmetry characteristic vibrational absorption patterns of CO ligands in the "naked" coordinatively unsaturated transition-metal carbonyls M(CO)$_{n-1}$ (M = Cr, Mo, and W; n = 4−6) observed by a time-resolved infrared absorption spectroscopy after the UV pulse laser photolysis of M(CO)$_6$ in the gas phase. The UV photolysis results can be reasonably explained by the trends in the calculated bond dissociation enthalpies of M(CO)$_{n-1}$−CO for group 6 metal carbonyls. M(CO)$_{n-1}$ produced through one CO elimination from M(CO)$_n$ is found out to keep its parent skeleton, resulting in the structure with symmetry of C_{4v} for M(CO)$_5$, C_{2v} for M(CO)$_4$, and C_{3v} for M(CO)$_3$.

Introduction

Coordinatively unsaturated transition-metal carbonyls not only play an important role in many homogeneous catalytic cycles but also give an instructive reaction field looked upon as transition-metal surface. The spectroscopic and structural studies of these transient species have been carried out by the UV photolysis of coordinatively saturated transition-metal carbonyls or by the matrix-isolation technique combined with the laser ablation of transition metals in the presence of CO.[1] Chemical reactivities of the "naked" coordinatively unsaturated sites have been investigated mainly using the time-resolved infrared absorption spectroscopy in the gas phase.[2]

Coordinatively unsaturated group 6 transition-metal carbonyls, M(CO)$_{n-1}$ (M = Cr, Mo, and W; n = 4−6), produced by the UV photolysis of M(CO)$_6$ show the characteristic infrared absorption patterns depending on the number of carbonyl ligand n in the CO stretching region.[3,4] By detailed ^{13}CO substitution studies in the low-temperature matrixes, Turner and co-workers showed that M(CO)$_5$ adopted a C_{4v} structure, M(CO)$_4$ a C_{2v} structure, and M(CO)$_3$ a C_{3v} structure.[4−6] The bond angle θ between the carbon of the unique CO (CO$_{ax}$) and the carbons of the basal CO molecules (CO$_{eq}$) in the C_{4v} Mo(CO)$_5$ were estimated to be between 90 and 95° by the infrared intensity analysis, and Mo(CO)$_4$ (C_{2v}) had two C−Mo−C angles of 174° and 107° and Mo(CO)$_3$ (C_{3v}) had an angle of 105°. The same symmetrical structures were proposed by the time-resolved infrared absorption spectroscopy in the gas phase.[7−10] However, the coordinatively unsaturated sites have been well-known to be so interactive, even with rare gas molecules, that the "naked" M(CO)$_{n-1}$ (n = 4−6) structure is expected to be more or less different from that of the M(CO)$_n$L$_{6-n}$ in the matrixes, where L is a matrix molecule. For example, the bond angle θ (C$_{ax}$−M−C$_{eq}$) (M = Cr, Mo, and W) of M(CO)$_5$ is estimated to be <90° by MP2 calculation,[11] which is not consistent with the experimental value of ≥90° for M(CO)$_5$L (L = Ar or CH$_4$).[6] It

* To whom correspondence should be addressed. E-mail: ishikawa@kit.ac.jp.
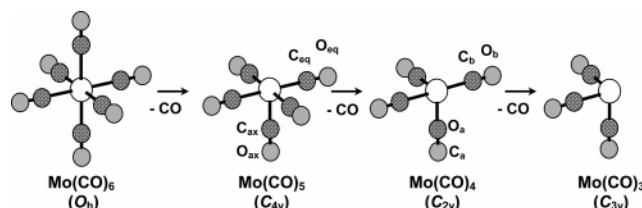
Figure 1. Optimized geometries of Mo(CO)$_6$, Mo(CO)$_5$, Mo(CO)$_4$, and Mo(CO)$_3$ by B3LYP with BS-1.

was pointed out that the weak interaction between M(CO)$_5$ and molecules L from the "inert" matrix might be responsible for such a conflict.[11]

In the primary process of UV photolysis of M(CO)$_6$, there has been an apparent difference between in the rigid phase and in the gas phase. In the rigid phase, only one CO elimination has been observed in spite of the photolysis wavelength, while the extent of the CO elimination has been observed to depend on the photolysis wavelength in the gas phase.[7−10] The observation results have been interpreted in terms of the fast intersystem crossing or the internal conversion in electronically excited M(CO)$_5$ fragment, followed by the thermal unimolecular decomposition on the singlet potential surface. The bimolecular rate constants for CO addition to M(CO)$_n$ (n = 2−5 for M = Cr and Mo and n = 4−5 for M = W) have been observed to be within an order of magnitude of the gas kinetic collision rate, also suggesting that the ground states of the M(CO)$_n$ have the singlet spin multiplicity similar to M(CO)$_6$.[10]

Density functional theory (DFT), using an appropriate basis set, has been recently reported to give a better description of not only the geometry but also the vibrational frequencies of transition-metal compounds.[1,11−15] Recently, these theoretical calculations have been successfully applied for the interpretation of the interaction between transition-metal center and ligands.[16−20] A systematical estimation of quantitative structure and M−CO bond dissociation enthalpy (BDE) of coordinatively unsaturated transition-metal carbonyls has been still interesting subjects.

DFT Studies of Group 6 Transition-Metal Carbonyls

J. Phys. Chem. A, Vol. 111, No. 39, 2007 **9941**

TABLE 1: Optimized Geometry of Cr(CO)$_n$ ($n = 3-6$) Calculated Using B3LYP with BS-1 and BS-2[a]

		this work		reported values	
		BS-1	BS-2	expt	calcd
Cr(CO)$_6$	r_1 (M−C)	1.920	1.927	1.914,[b] 1.916[c]	1.8827,[d] 1.908[e]
	r_2 (C−O)	1.139	1.140	1.140,[b] 1.140[c]	1.1678,[d] 1.154[e]
Cr(CO)$_5$	r_1 (M−C$_{ax}$)	1.848	1.856		1.7735[d]
	r_2 (C$_{ax}$−O$_{ax}$)	1.147	1.147		1.1934[d]
	r_3 (M−C$_{eq}$)	1.922	1.928		1.8913[d]
	r_4 (C$_{eq}$−O$_{eq}$)	1.141	1.141		1.1663[d]
	A_1 (C$_{eq}$−M−C$_{ax}$)	90.67	90.81		86.0[d]
	A_2 (M−C$_{eq}$−O$_{eq}$)	178.0	178.3		173.4[d]
Cr(CO)$_4$	r_1 (M−C$_a$)	1.839	1.844		
	r_2 (C$_a$−O$_a$)	1.149	1.150		
	r_3 (M−C$_b$)	1.921	1.925		
	r_4 (C$_b$−O$_b$)	1.142	1.143		
	A_1 (C$_a$−M−C$_a$)	90.86	91.23		
	A_2 (C$_b$−M−C$_b$)	179.5	179.7		
	A_1 (M−C$_a$−O$_a$)	179.5	179.7		
	A_2 (M−C$_b$−O$_b$)	176.0	176.2		
Cr(CO)$_3$	r_1 (M−C)	1.828	1.829		
	r_2 (C−O)	1.153	1.154		
	A_1 (C−M−C)	90.19	90.19		
	A_2 (M−C−O)	178.6	178.7		

[a] Geometrical symbols used here are shown in Figure 1. (r in Å and A in degree (°)). [b] Neutron diffraction, ref 26. [c] X-ray, ref 27. [d] MP2/basis set IV, ref 11. [e] BP86/basis set ECP2, ref 12.

In this paper, the geometries of M(CO)$_n$ (M = Cr, Mo, and W; $n = 3-6$) optimized using DFT are reported. The DFT methodology is selected to reproduce the characteristic vibrational patterns observed by a transient infrared absorption spectroscopy in the gas phase.[9,21,22] The calculation results are used to estimate the BDEs of M(CO)$_{n-1}$−CO and to discuss the UV photolysis mechanisms of M(CO)$_6$ in the gas phase.

Calculation Details

DFT (B3LYP) calculations were carried out on all related transition-metal carbonyls using Gaussian 03W program.[23] Basis set composed of 6-311+G(2d) functions on carbon and oxygen atoms and LANL2DZ basis function with ECP on transition-metal atoms (abbreviated to "BS-1" hereafter) was used in combination with B3LYP calculation. All-electron basis function of 6-311+G(2d) ("BS-2") was used only for Cr(CO)$_n$ if necessary. The 6-311+G(2d) basis function on C and O atoms was chosen because it gave a more reasonable vibrational frequency result (2055 cm^{-1}) for the T_{1u} CO-stretching mode of W(CO)$_6$ among STO-3G (2077 cm^{-1}), 6-31G(d) (2075 cm^{-1}), 6-31+G(d) (2058 cm^{-1}), 6-311G(d) (2069 cm^{-1}), 6-311+G(2df) (2059 cm^{-1}), 6-311+G(3df) (2059 cm^{-1}), and 6-311+G(2d). Full geometry optimization without any symmetry constraints has been carried out first, starting from several initial geometries. The final geometry optimization was executed with the resultant symmetry constraint.

The calculated vibrational frequencies and the moments of inertia of M(CO)$_n$ at optimized geometry were used in the estimation of the dissociation enthalpy (BDE$_n$) between M(CO)$_{n-1}$ and CO at 298 K, which was estimated using the expression:

$$\Delta H_{298}(\text{BDE}_n) = \Delta E_c + \Delta \text{ZPE} + \Delta E_{th} + \Delta(PV)$$

where ΔE_c was the difference in the optimized energies of the reactant (M(CO)$_n$) and the product (M(CO)$_{n-1}$ + CO), ΔZPE was the zero point energy correction obtained from the calculation of vibrational frequencies, ΔE_{th} was the difference associated with the translational, rotational, and vibrational energy at
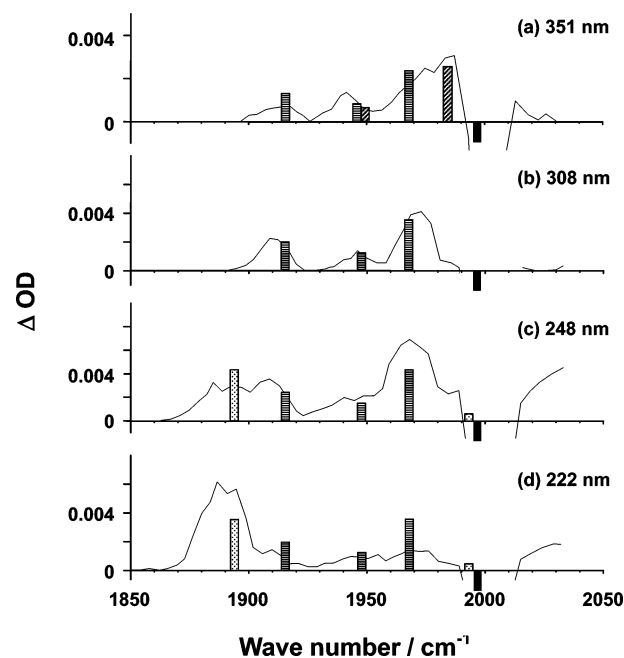

Figure 2. Comparison of the infrared difference absorption spectrum observed in the gas phase and the vibrational frequencies (ν_{corr}) calculated for Mo(CO)$_n$ (Mo(CO)$_6$ represented as a black rectangle, Mo(CO)$_5$ as slant-line hatched rectangles, Mo(CO)$_4$ as horizontal-line hatched rectangles, and Mo(CO)$_3$ as dot hatched rectangles). The height of each rectangle reflects a relative absorption intensity ratio for each Mo(CO)$_n$ compound. The ordinate scale ΔOD indicates the difference optical density between before and at 1.0 μs after XeF laser photolysis (a; $\lambda = 351$ nm), after XeCl laser photolysis (b; $\lambda = 308$ nm), after KrF laser photolysis (c; $\lambda = 248$ nm), and after KrCl laser photolysis (d; $\lambda = 222$ nm) of Mo(CO)$_6$ (~20 mTorr) at a total pressure of 6.0 Torr with balance Ar.

0 and 298 K, and $\Delta(PV)$ was the molar work equal to ΔnRT in the gas-phase reaction.[24,25]

Results and Discussion

Figure 1 shows the optimized geometries of Mo(CO)$_6$, Mo(CO)$_5$, Mo(CO)$_4$, and Mo(CO)$_3$ by B3LYP with BS-1. The other two transition-metal carbonyls, Cr(CO)$_n$ and W(CO)$_n$, have very similar optimized structures, which are summarized in Tables 1 (Cr(CO)$_n$) and 2 (Mo(CO)$_n$ and W(CO)$_n$) together with the previous experimental and theoretical results. In the case of Cr(CO)$_n$, the optimization was also carried out using B3LYP with all-electron basis function sets on Cr (BS-2). The optimization results with BS-2 shown in Table 1 seem to be consistent with those calculated using BS-1, suggesting that the ECP of LANL2DZ works well in the case of Cr atom. All values calculated for M(CO)$_6$ by B3LYP/BS-1 are also within the experimental errors reported (Cr: r(Cr−C) = 1.92 ± 0.04 Å and r(C−O) = 1.16 ± 0.05 Å; Mo: r(Mo−C) = 2.08 ± 0.04 Å and r(C−O) = 1.15 ± 0.05 Å; W: r(W−C) = 2.06 ± 0.04 Å and r(C−O) = 1.13 ± 0.05 Å).[30] The naked transition-metal carbonyl M(CO)$_{n-1}$ produced through one CO elimination from M(CO)$_n$ keeps its residual parent skeleton, resulting in the structure with symmetry of C_{4v} for M(CO)$_5$, C_{2v} for M(CO)$_4$, and C_{3v} for M(CO)$_3$. These structural symmetries are almost consistent with the previous observations[4,7,8,31−33] and calculations.[34−36] The spin multiplicity in the ground electronic state of M(CO)$_n$ ($n = 3-5$) was singlet for all compounds. In the gas phase, the coordinatively unsaturated transition-metal carbonyls M(CO)$_n$ ($n = 3-5$) have been observed to react with CO nearly at the gas kinetic collision rate, suggesting that all M(CO)$_n$'s have the same singlet spin to M(CO)$_6$.

TABLE 2: Optimized Geometry of M(CO)$_n$ (M = Mo and W, n = 3−6) Calculated Using B3LYP with BS-1[a]

		Mo			W		
		this work	reported values		this work	reported values	
			expt	calcd		expt	calcd
M(CO)$_6$	r_1 (M−C)	2.084	2.063[b]	2.0659[d]	2.071	2.058[b]	2.0534[d]
			2.059[c]	2.065[e]			2.075[e]
	r_2 (C−O)	1.139	1.145[b]	1.1644[d]	1.141	1.148[b]	1.1659[d]
			1.125[c]	1.153[e]			1.154[e]
M(CO)$_5$	r_1 (M−C$_{ax}$)	1.959		1.9352[d]	1.955		1.9353[d]
	r_2 (C$_{ax}$−O$_{ax}$)	1.149		1.1783[d]	1.152		1.1785[d]
	r_3 (M−C$_{eq}$)	2.078		2.0631[d]	2.063		2.0490[d]
	r_4 (C$_{eq}$−O$_{eq}$)	1.140		1.1652[d]	1.142		1.1676[d]
	A_1 (C$_{eq}$−M−C$_{ax}$)	89.63		86.9[d]	90.40		86.84[d]
	A_2 (M−C$_{eq}$−O$_{eq}$)	177.9		175.0[d]	178.7		175.3[d]
M(CO)$_4$	r_1 (M−C$_a$)	1.946			1.939		
	r_2 (C$_a$−O$_a$)	1.152			1.155		
	r_3 (M−C$_b$)	2.071			2.053		
	r_4 (C$_b$−O$_b$)	1.142			1.145		
	A_1 (C$_a$−M−C$_a$)	88.17			88.89		
	A_2 (C$_b$−M−C$_b$)	177.6			179.8		
	A_1 (M−C$_a$−O$_a$)	179.4			179.8		
	A_2 (M−C$_b$−O$_b$)	176.4			177.6		
M(CO)$_3$	r_1 (M−C)	1.930			1.921		
	r_2 (C−O)	1.156			1.159		
	A_1 (C−M−C)	87.77			88.65		
	A_2 (M−C−O)	178.9			179.5		

[a] Geometrical symbols used here are shown in Figure 1. (r in Å and A in degree (°)). [b] Electron diffraction, ref 28. [c] X-ray, ref 29. [d] MP2/basis set IV, ref 11. [e] BP86/basis set ECP2, ref 12.

The ground state of M(CO)$_5$ has a square pyramid structure C_{4v} with the angle C$_{eq}$−M−C$_{ax}$ of ca. 90°. M(CO)$_5$ structure was checked not to be optimized in constraint of trigonal bipyramid D_{3h} symmetry. The triplet state of Mo(CO)$_5$ with D_{3h} symmetry of trigonal bipyramid was optimized to be located at 25.8 kcal mol^{-1} (ΔE_c) above the singlet ground state (13.0 kcal mol^{-1} for Cr(CO)$_5$ and 21.5 kcal mol^{-1} for W(CO)$_5$). The singlet state of M(CO)$_4$ was optimized to have a C_{2v} structure and to have two C−M−C angles of ca. 180° and ca. 90°. The triplet state with a compressed tetrahedral structure (C_{2v}) was located at 25.1 kcal mol^{-1} above the singlet ground states for Cr(CO)$_4$ (7.8 kcal mol^{-1} for Cr(CO)$_4$ and 23.1 kcal mol^{-1} for W(CO)$_4$). Mo(CO)$_4$ with a planar D_{4d} symmetry was located at 23 kcal mol^{-1} higher than the ground state (10 kcal mol^{-1} for Cr(CO)$_4$ and 28 kcal mol^{-1} for W(CO)$_4$). The optimized structure of M(CO)$_3$ was a C_{3v} symmetry with an angle of ca. 90°. A T-shape structure was suggested for the triplet state of Mo(CO)$_3$, which was located only at 24 kcal mol^{-1} above the singlet ground state (3 kcal mol^{-1} for Cr(CO)$_3$ and 21 kcal mol^{-1} for W(CO)$_3$).

A stability of Cr(CO)$_5$ for equatorial-axial exchange was studied by B3LYP based DFT calculations with 6-311+G(2d) basis function. The transition state of this exchange was found to have a C_{2v} symmetry as shown below, which lay at
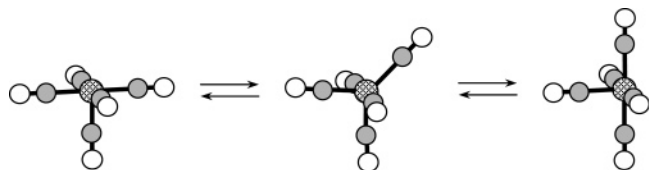
12.7 kcal mol^{-1} higher than the ground C_{4v} structure in E_c. A D_{3d} trigonal bipyrimad (TBP) could not be a structure of transition state in this mechanism.

Figure 2 shows a comparison between experimental (ν_{obs})[9] and theoretical (ν_{corr}) frequencies of the CO-stretching modes
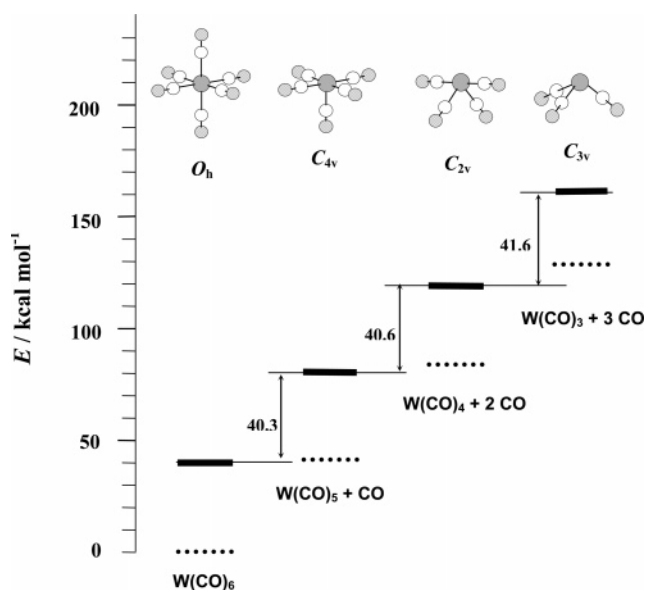
**Figure 3.** Schematic energy diagram in which the electronic energy difference to W(CO)$_6$ is represented as a dotted line and the enthalpy difference as a solid line. The calculated bond enthalpy for each CO elimination reaction is in kcal mol^{-1} and the optimized schematic geometries for W(CO)$_6$, W(CO)$_5$, W(CO)$_4$, and W(CO)$_3$ are also shown.

of Mo(CO)$_n$ (n = 3−6). As the observed fundamental frequency (ν_{obs}) is usually lower than the harmonic frequency (ω_e) by about $2\omega_e\chi_e$ ($\omega_e\chi_e$ is an anharmonicity constant in cm^{-1}), the observed fundamental frequency (ν_{obs}) and the harmonic frequency calculated by DFT theory (ω_{cal}) are not comparable without the accurate knowledge of an anharmonicity. An appropriate, generally accepted correction was made for the calculated harmonic frequency (ω_{cal}) to estimate the theoretical fundamental frequency (ν_{corr}) by multiplying ω_{cal} with a scaling factor (λ = 0.9679).[37] The transient infrared absorption difference spectra in the 1850−2050 cm^{-1} were observed at 1 μs after

DFT Studies of Group 6 Transition-Metal Carbonyls

J. Phys. Chem. A, Vol. 111, No. 39, 2007 **9943**

TABLE 3: Comparison between Experimental Vibrational Frequencies (ν_{obs}) and Theoretical Ones (ν_{corr} and ω_{cal}) Calculated Using B3LYP with BS-1 for the Gas-Phase C−O Stretching Frequencies (in cm^{-1}) of M(CO)$_n$ (M = Cr, Mo, and W; $n = 3-6$)

			Cr			Mo			W		
			$\nu_{obs}{}^a$ (int)^e	$\nu_{corr}{}^b$ (int)^f	ω_{cal}	$\nu_{obs}{}^c$ (int)^e	$\nu_{corr}{}^b$ (int)^f	ω_{cal}	$\nu_{obs}{}^d$ (int)^e	$\nu_{corr}{}^b$ (int)^f	ω_{cal}
M(CO)$_6$	O_h	T_{1u}	1999	1999 [1993]^g	2065 [2059]^g	2000	1996	2062	1999	1989	2055
M(CO)$_5$	C_{4v}	E	1976 (1.0)	1983 [1978]^g (1.00)	2049 [2043]^g	1990 (1.0)	1984 (1.00)	2050	1980 (1.0)	1973 (1.00)	2038
		A_1	1950 (∼0.3)	1962 [1956]^g (0.21)	2027 [2021]^g	1942 (∼0.3)	1948 (0.22)	2013	1942 (∼0.2)	1942 (0.22)	2006
M(CO)$_4$	C_{2v}	B_1	1954 (1.0)	1969 [1960]^g (1.00)	2034 [2026]^g	1972 (1.0)	1968 (1.00)	2033	1957 (1.0)	1954 (1.00)	2019
		A_1		1958 [1950]^g (0.26)	2023 [2015]^g	1946 (∼0.3)	1948 (0.28)	2013	1942 (∼0.3)	1948 (0.29)	2004
		B_2	1916 (∼0.4)	1935 [1927]^g (0.54)	1999 [1990]^g	1911 (∼0.5)	1916 (0.53)	1980	1909 (∼0.5)	1915 (0.54)	1971
M(CO)$_3$	C_{3v}	A_1		2002 [1993]^g (0.09)	2068 [2059]^g		1993 (0.13)	2059		1994 (0.13)	2050
		E	1887	1915 [1899]^g (1.00)	1979 [1962]^g	1891	1893 (1.00)	1956	1887	1887 (1.00)	1943

^{a} Reference 21. ^{b} $\nu_{corr} = \lambda \times \omega_{cal}$ ($\lambda = 0.9679$; scaling factor^{37}). ^{c} Reference 9. ^{d} Reference 22. ^{e} Experimental absorption peak intensity ratios for each compound in parentheses. These ratios are rough owing to the spectrum overlaps. ^{f} Calculated intensity ratios for each compound in parentheses. ^{g} Frequencies calculated by B3LYP with BS-2 are shown in square brackets.

TABLE 4: M(CO)$_{n-1}$−CO Bond Dissociation Enthalpies, BDE$_n$/kcal mol^{-1}, in Group 6 M(CO)$_n$ Species Calculated Using B3LYP with BS-1

		Cr	Mo	W
BDE$_6$	this work	32.8 [33.8]^a	32.0	40.3
	expt	37 ± 2,^{b} 37 ± 5,^{c} 37 ± 5^d	40 ± 2,^{b} 34 ± 5^d	46 ± 2,^{b} 38 ± 5^d
	calcd	45.3,^{e} 35.1^f	40.3,^{e} 28.4^f	47.8,^{e} 33.9^f
BDE$_5$	this work	32.0 [33.5]^a	31.7	40.6
	expt	25 ± 5,^{c} 33,^{g} 25 ± 5^h	29.5,^{g} 35 ± 5^h	36−39,^{g} 40 ± 15^h
BDE$_4$	this work	33.3 [34.2]^a	32.1	41.6
	expt	39,^{g} 20 ± 15^h	31,^{g} 30 ± 15^h	>33,^{g} 25 ± 5^h
BDE$_{av}$	expt	25.8^i	36.3^i	42.5^i
	calcd	25.6^f	30.1^f	37.3^f

^{a} Calculated values using all-electron basis function set (6-311+G(2d)) for Cr are shown in square parentheses. ^{b} Reference 38. ^{c} Reference 39. ^{d} Reference 40. ^{e} CCSD(T)/II, ref 11. ^{f} DFT/NL, ref 41. ^{g} Reference 42. ^{h} Reference 43. ^{i} Reference 44.

photolysis when Mo(CO)$_6$ (vapor pressure ∼ 10 mTorr) in ∼5 Torr of Ar buffer gas photolyzed at different excimer laser wavelengths at room temperature.^{9} The reasonable coincidence of the two absorption patterns in the two frequencies (ν_{obs} and ν_{corr}) and in the relative peak intensities supports the previous interpretation of the photon energy dependence of fragment distribution in Mo(CO)$_6$ UV photolysis.^{9} In 351 nm photolysis (a, XeF laser), two fragments of Mo(CO)$_5$ and Mo(CO)$_4$ are produced to the similar extent while Mo(CO)$_4$ is found out to be a main fragment in 308 nm photolysis (b, XeCl laser). In 248 nm photolysis (c, KrF laser), a primary fragment is Mo-(CO)$_4$ and a secondary fragment is Mo(CO)$_3$ on the assumption that the peak infrared absorption coefficients of Mo(CO)$_4$ (B_1) and Mo(CO)$_3$ (E) are the same. The equivalence in the infrared absorption coefficient was approximately suggested by the DFT calculation. A main fragment is Mo(CO)$_3$ and a trace of Mo-(CO)$_4$ is seen in 222 nm photolysis (d, KrCl laser). The C−O stretching frequencies for M(CO)$_n$ observed to date and

calculated in this study are summarized in Table 3. All-electron basis function 6-311+G(2d) (BS-2) on the transition-metal atom was used only in case of Cr(CO)$_6$. Comparison of the calculated (ν_{corr}) and the observed (ν_{obs}) frequencies seems to give reasonable agreement for all transition-metal carbonyl compounds, suggesting that the DFT calculation can simulate well the interaction between transition-metal center and CO ligand and the structure.

Figure 3 shows the schematic energy diagram related to the electronic energy of W(CO)$_n$ ($n = 3-6$) (dotted lines) and the enthalpy (solid lines) for each CO elimination reaction at 298 K, which was constructed from the DFT calculation using B3LYP with BS-1. Table 4 shows the result for the bond dissociation enthalpy (BDE$_n$) at 298 K. The BDE$_n$'s are in the order of W > Cr > Mo for $n = 4-6$, though the difference between Cr and Mo is fairly small. This tendency in BDE$_n$ is consistent with the fragmentary extent in UV photolysis. At 222 nm photolysis, W(CO)$_6$ eliminates only two COs to form

$W(CO)_4$ while both $Cr(CO)_6$ and $Mo(CO)_6$ eliminate three COs at least. The main fragment of $Mo(CO)_6$ is $Mo(CO)_3$ while $Cr(CO)_4$ is produced in the similar extent to $Cr(CO)_3$ in 222 nm photolysis. For UV photolysis, a labile group 6 transition-metal carbonyl seems to be $Mo(CO)_6$.

Conclusion

The B3LYP-based calculation with ECPs (LANL2DZ) on M (M = Cr, Mo, and W) and 6-311+G(2d) all-electron basis sets on C and O could well reproduce the absorption frequency and the symmetry characteristic vibrational patterns of CO coordinated in $M(CO)_n$. The results of the structural optimization of $M(CO)_n$ ($n = 3-6$) suggest that $M(CO)_{n-1}$ keeps its parent skeleton in $M(CO)_{n-1} - CO$ dissociation process, resulting in the structure with symmetry of C_{4v} for $M(CO)_5$, C_{2v} for $M(CO)_4$, and C_{3v} for $M(CO)_3$ as shown in Figure 1. The BDE_n's are in the order of W > Cr > Mo for $n = 4-6$, though the difference between Cr and Mo is fairly small.

References and Notes

(1) Zhou, M.; Andrews, L.; Bauschlicher, C. W., Jr. *Chem. Rev.* **2001**, *101*, 1931.

(2) Weitz, E. *J. Phys. Chem.* **1994**, *98*, 11256.

(3) Orgel, L. E. *Inorg. Chem.* **1962**, *1*, 25.

(4) Perutz R. N.; Turner, J. J. *J. Am. Chem. Soc.* **1975**, *17*, 4800.

(5) Graham, M. A.; Poliakoff, M.; Turner, J. J. *J. Chem. Soc. A* **1971**, 2940.

(6) Perutz, R. N.; Turner, J. J. *Inorg. Chem.* **1975**, *14*, 262.

(7) Seder, T. A.; Church, S. P.; Weitz, E. *J. Am. Chem. Soc.* **1986**, *108*, 4721.

(8) Fletcher, T. R.; Rosenfeld, R. N. *J. Am. Chem. Soc.* **1985**, *107*, 2203.

(9) Ishikawa, Y.; Brown, C. E.; Hackett, P. A.; Rayner, D. M. *J. Phys. Chem.* **1990**, *94*, 2404.

(10) Weitz, E. *J. Phys. Chem.* **1987**, *91*, 3945.

(11) Ehlers, A. W.; Frenking, G. *J. Am. Chem. Soc.* **1994**, *116*, 1514.

(12) Jones V.; Thiel, W. *J. Chem. Phys.* **1995**, *102*, 8474.

(13) Frenking, G.; Pidum, U. *J. Chem. Soc., Dalton Trans.* **1997**, 1653.

(14) Ricca, A.; Bauschlicher, C. W., Jr. *Theor. Chim. Acta* **1995**, *92*, 123.

(15) Glukhovtsev, M. N.; Bach, R. D.; Nagel, C. J. *J. Phys. Chem. A* **1997**, *101*, 316.

(16) Ehlers, A. W.; Frenking, G.; Baerends, E. J. *Organometallics* **1997**, *16*, 4896.

(17) Shanoski, J. E.; Payne, C. K.; Kling, M. F.; Glascoe, E. A.; Harris, C. B. *Organometallics* **2005**, *24*, 1852.

(18) Jaeger, T. D.; Duncan, M. A. *J. Phys. Chem. A* **2005**, *109*, 3311.

(19) Kovacs, A.; Frenking, G. *Organometallics* **2001**, *20*, 2510.

(20) Nechaev, M. S.; Rayon, V. M.; Frenking, G. *J. Phys. Chem. A* **2004**, *108*, 3134.

(21) Weitz, E. *J. Phys. Chem.* **1987**, *91*, 3945.

(22) Ishikawa, Y.; Hackett, P.; Rayner, D. M. *J. Phys. Chem.* **1988**, *92*, 3863.

(23) Frisch, M. J. et al. *Gaussian 03* (Revision B.05); Gaussian, Inc.: Pittsburgh, PA, 2003.

(24) Foresman, J. B.; Frisch, A. *Exploring Chemistry with Electronic Structure Methods*; Gaussian, Inc.: Pittsburgh, PA, 1996; p 47.

(25) Cedeño, D. L.; Weitz, E.; Berces, A. *J. Phys. Chem. A* **2001**, *105*, 8077.

(26) Jost, A.; Rees, B.; Yelon, W. B. *Acta Crystallogr., Sect. B* **1975**, *31*, 2649.

(27) Rees, B.; Mitschler, A. *J. Am. Chem. Soc.* **1976**, *98*, 7918.

(28) Arnesen, S. V.; Seip, H. M. *Acta Chem. Scand.* **1966**, *20*, 2711.

(29) Mak, T. C. W. *Z. Kristallogr.* **1984**, *166*, 277.

(30) Wender, I.; Piero, P. *Orgnic Syntheses via metal carbonyls*; Interscience Publishers: New York, 1968; Vol. 1.

(31) Burdett, J. K.; Graham, M. A.; Perutz, R. N.; Poliakoff, M.; Rest, A. J.; Turner, J. J.; Turner, R. F. *J. Am. Chem. Soc.* **1975**, *97*, 4085.

(32) Graham, M. A.; Poliakoff, M.; Turner, J. J. *J. Am. Chem. Soc.* **1975**, *97*, 4085.

(33) Ishikawa, Y.; Hackett, P. A.; Rayner, D. M. *J. Phys. Chem.* **1988**, *92*, 3863.

(34) Hay, P. J. *J. Am. Chem. Soc.* **1978**, *100*, 2411.

(35) Rosa, A.; Ehlers, A. W.; Baerends, E. J.; Snijders, J. G.; te Velde, G. *J. Phys. Chem.* **1996**, *100*, 5690.

(36) Barnes, L. A.; Liu, B.; Lindh, R. *J. Chem. Phys.* **1993**, *98*, 3978.

(37) Andersson, M. P.; Uvdal, P. *J. Phys. Chem. A* **2005**, *109*, 2937.

(38) Lewis, K. E.; Golden, D. M.; Smith, D. M. *J. Am. Chem. Soc.* **1984**, *106*, 3905.

(39) Fletcher, T. R.; Rosenfeld, R. N. *J. Am. Chem. Soc.* **1988**, *110*, 2097.

(40) Bernstein, M.; Simon, J. D.; Peters, J. D. *Chem. Phys. Lett.* **1983**, *100*, 241.

(41) Ziegler, T.; Tschinke, V.; Ursenbach, C. *J. Am. Chem. Soc.* **1987**, *109*, 4825.

(42) Rayner, D. M.; Ishikawa, Y.; Brown, C. E.; Hackett, P. A. *J. Chem. Phys.* **1991**, *94*, 5471.

(43) Venkataraman, B.; Hou, H.; Zhang, Z.; Chen, S.; Bandukwalla, G.; Vernon, M. *J. Chem. Phys.* **1990**, *92*, 5338.

(44) Connor, J. A. *Top. Curr. Chem.* **1977**, *71*, 71.